High Temperatures-High Pressures, Vol. 45, pp. 255–271
Reprints available directly from the publisher
Photocopying permitted by license only

Heat balance in levitation melting: Sample cooling by forced gas convection in Argon

GEORG LOHÖFER* AND STEPHAN SCHNEIDER

Institut für Materialphysik im Weltraum, Deutsches Zentrum für Luft- und Raumfahrt (DLR), 51170 Köln, Germany

Received: January 18, 2016. Accepted: February 10, 2016.

Electromagnetic levitation melting is a containerless processing technique for liquid metals requiring non-contact diagnostic tools. In order to properly perform such experiments, a precise knowledge of the temperature-time behaviour of the metal sample resulting from the heat balance between its heating and cooling during the processing is a prerequisite. In two preceding papers we provided the necessary theoretical background for the inductive heat input by the high frequency magnetic levitation field and the heat loss due to radiation and heat conduction through a surrounding process gas atmosphere and defined the set of experiments needed for obtaining the key parameters of the thermal model. In the present paper we extend the previous work by investigating experimentally the influence of the sample cooling by forced gas convection at high Péclet number in a surrounding Argon gas atmosphere at hand of tests under microgravity.

Keywords: Containerless processing, Electromagnetic levitation, Forced convection, Heat balance, Microgravity

1 INTRODUCTION

The present work is the fourth one in a series of publications [1, 2, 3] investigating on the basis of the energy balance between heating and cooling the temperature-time behaviour of a metal sample processed containerlessly in an electromagnetic levitation facility. It is motivated by the fact, that electromagnetic levitation is a widely-used, simple and robust method for the

*Corresponding author: Georg.Lohoefer@dlr.de

containerless, and thus mechanically and chemically unaffected, handling of hot metallic melts during the measurement of their thermophysical properties or the study of their solidification behaviour [4, 5].

This technique applies inhomogeneous, high frequency (≈300 kHz) electromagnetic fields, which are generated by alternating currents flowing through suitably shaped levitation coils, to induce eddy currents in a small (≈6 mm diameter) metallic specimen inside the coil. Together with the original magnetic fields these eddy currents generate a Lorentz force which levitates the metal against earth's gravity. Furthermore, the eddy currents heat and melt the specimen due to resistive losses [4].

Performed in the essentially forceless, so called "microgravity" (μg) environment, which is realised within the ≈20 seconds lasting free fall time during parabolic flights of aircrafts [6], within the ≈5 minutes lasting free fall time during sounding rocket missions or without time limit inside the "International Space Station" (ISS) [7], electromagnetic levitation offers several additional advantages. Under this condition the lifting force can strongly be

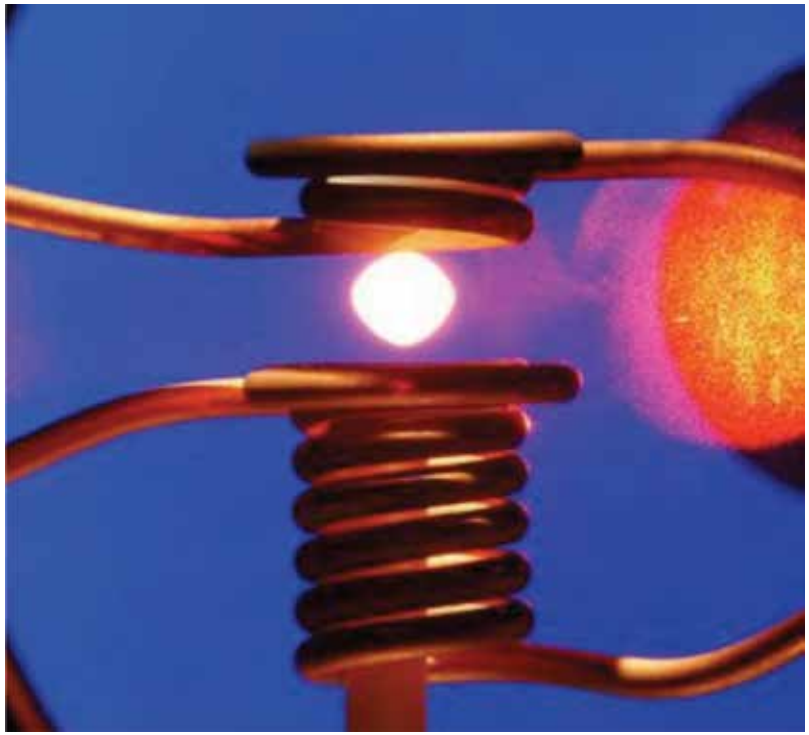

FIGURE 1
Picture of a liquid, levitated metal sample enclosed by the alternating current carrying levitation coil on ground. The coil consists of a water cooled copper tube.

reduced, and heating and positioning of the sample can be performed independently by two superposed magnetic fields [8]. Furthermore, the resulting spherical shape and the absence of the gravity driven free convection of the surrounding gas atmosphere simplifies the modelling of the energy balance of the levitated sample. For all of the above mentioned carriers the "German Aerospace Center" (DLR) or the "European Space Agency" (ESA) provide dedicated electro magnetic levitation facilities, which are all very similar as far as the heating and cooling conditions for the levitated samples are concerned. In order to properly perform such an experiment procedure in these facilities, a precise prediction of the sample temperature on the basis of the heat balance between heating and cooling of the sample is a prerequisite, especially if the processing is performed fully automated and remotely.

In a preceding paper [1] we already provided the necessary theoretical background for the inductive heat input by the high frequency magnetic levitation fields and the heat loss due to radiation and, if carried out in a gas atmosphere, heat conduction through the surrounding gas. In a second paper [2] we extended and partly improved the previous work by detailed investigations of the influence of the sample cooling by pure heat conduction in an static Argon and Helium process atmosphere. In a third paper [3] we studied the heat balance of a sample under the additional influence of a forced convection cooling in a Helium and Argon gas atmosphere. During this investigation it turned out, that the basic physical model derived in [3] fits very well to the measured forced convection cooling in the thermally well conducting Helium atmosphere, but could not simply be transferred to the convection cooling in the poorly heat conducting Argon atmosphere.

The subject of the present work is therefore the experimental study of the heat balance of a sample under the additional influence of a forced convection cooling in an Argon gas flow on the basis of a physical model derived in [9]. This study has been performed with a solid, spherical test sample of pure Zirconium levitated in the "TEMPUS" parabolic flight facility during several parabolas, flown on board the "zero-g" aircraft of "Novespace" [6]. Each parabola provided a reduced ($\approx$1/100) sample weight within a time span of $\approx$20 seconds. Pure Zirconium has the advantage, that its $\alpha \rightarrow \beta$ phase transition in the solid state at 1142 K is well recognizable in the pyrometrically measured temperature signal and can therefore simultaneously also be used for a calibration of this signal.

2 EXPERIMENTAL SITUATION

During the 25th DLR parabolic flight campaign in October 2014 a pure (99.97%) solid Zirconium sphere of 7.0 mm diameter has been processed in the centre of the levitation coils of the microgravity levitation facility TEMPUS, as schematically shown in Figure 2. In the course of the $\approx$20 seconds

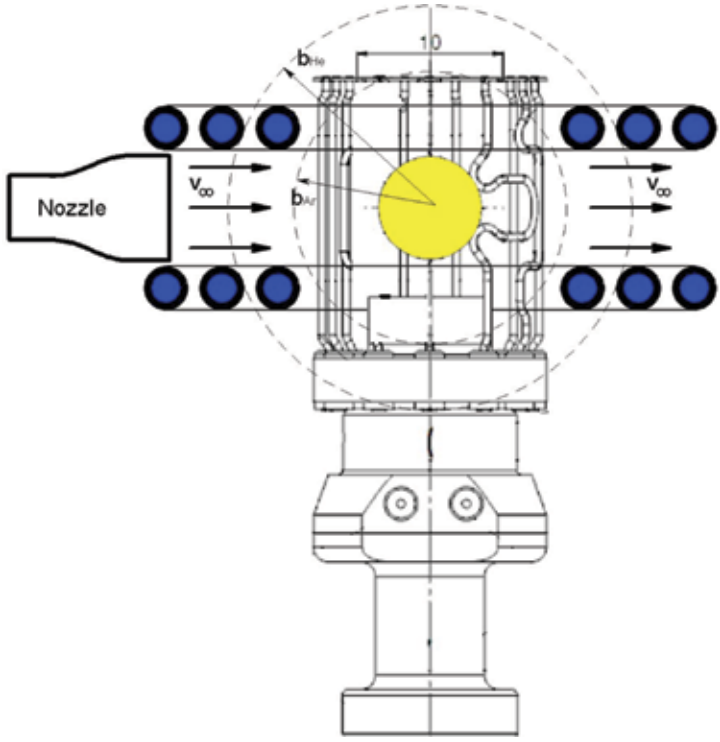

FIGURE 2
Sketch of the Zr test sample (yellow) enclosed in a cage and levitated by the high frequency magnetic fields of TEMPUS between the horizontal, circular magnetic coil windings (black circles). The heat in the sample, inductively generated by the magnetic fields, is absorbed by the internally water cooled copper coils, the thermally well conducting silicon nitride ceramic pedestal of the cage and the process chamber walls. The arrows indicate the flow of the cooling gas around the sample.

lasting low gravity phase of the parabolic flight the following three process steps, illustrated exemplarily by the temperature-time diagram of Fig. 3, were performed with the Zr-sphere under different atmospheric conditions in the process chamber.

1. Contactless positioning of the sample in the centre of the levitation coil by the quadrupole shaped high frequency magnetic "positioning field" [1].
2. Inductive heating of the sample to about 1650K ($T_{\text{melt}} = 2125$K) by the additional high frequency dipole shaped magnetic "heating field" [1].
3. Deactivation of the heating field and reduction of the positioning field, so that the liquid sample cools freely down. During this phase of minimal external impact the different experiments at the sample are performed.

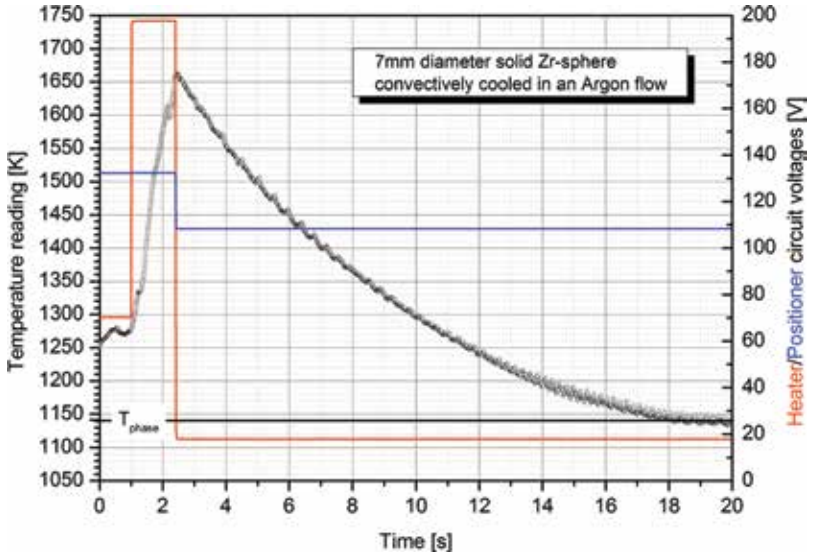

FIGURE 3
Typical temperature-time profile (black circles) as well as heater (red line) and positioner (blue line) circuit voltages of a solid $\varnothing = 7$ mm Zirconium sphere processed in TEMPUS in an Argon gas flow during the ≈20s µg time of a parabola. The three process phases can well be identified by the heater circuit voltages and the resulting sample temperature data. The temperature plateau around the 19th second indicates the solid-solid phase transition of the Zirconium sample at 1142 K.

The experiment time was just long enough for the sample to reach in the cooling Argon gas flow its solid phase transition temperature at 1142K, which is used as calibration point for the contactless pyrometric temperature measurement. During 5 parabolas, the following 5 different cooling conditions for the spherical Zr test sample have been set:

1st Parabola:	Cooling in vacuum
2nd – 5th Parabola:	Cooling in the Argon atmosphere with an additional gas flow, driven by a circulation pump at 4 different motor voltages, respectively.

- During all 5 experiment cycles the pressure of the Argon atmosphere in the process chamber was 350 ± 2 mbar.
- During all cooling cycles the voltage generating the magnetic positioning field has constantly been set to 108V and the voltage generating the magnetic heating field to 18V, so that the induced power from the magnetic levitation fields was always the same.
- Due to the weightlessness during the sample cooling phase gravity driven natural convection cooling in the surrounding gas could be neglected.

The relevant properties of the solid Zirconium test sphere of 99.97% purity were [10]:

- Melting temperature: $T_M = 2125K$.
- Solid phase transition temperature: $T_{phase} = 1142K$.
- Mean specific heat in the solid between $1200K < T < 1600K$: $c_p = 0.334$ *[Ws/(gK)]*.
- Sample mass: $m = 1.17\ g$.
- Sample radius: $a = 3.50\ mm$.

3 PHYSICAL BASICS

The basis for the temperature behaviour of the sample inside the TEMPUS facility is provided by the heat balance equation

$$\frac{dE(t)}{dt} = m\,c_p\,\frac{dT(t)}{dt} = P^{ind}(t) - P^{rad}(T(t)) - P_{gas}(T(t)) \tag{1}$$

with

$$P_{gas}(T) := P_{gas}^{con}(T) + P_{gas}^{flow}(T), \tag{2}$$

the detailed derivation of which is described in [1]. The internal energy change dE/dt of the levitated material results in a time dependent temperature change dT/dt depending on the temperature T, the mass m, and the specific heat c_p of the spherical isothermal sample. The considered external power in- and output is due to

- P^{ind}, which denotes the **inductive heat transfer** from both high frequency electromagnetic levitation fields of TEMPUS to the sample. P^{ind} was the same during all cooling phases.
- $P^{rad}(T)$, which denotes the temperature dependent **radiative heat transfer** between the sample and its environment (sample holder, coil, process chamber walls). Since the sample surface and the environment remained always the same, this function did not change during all cooling phases.
- $P_{gas}^{con}(T)$, which denotes the temperature dependent heat transfer between the sample and its environment (sample holder, coil, process chamber walls) solely by **heat conduction** through the static surrounding gas atmosphere. Since for the same atmosphere the environment remained always the same, this function did not change during the corresponding cooling cycles.
- $P_{gas}^{flow}(T)$, which denotes the temperature dependent heat transfer between the sample and its environment (sample holder, coil, process chamber walls) solely by **forced convection** in the surrounding gas atmosphere.

Whereas the functions P^{ind} , $P^{rad}(T)$ and $P^{con}_{gas}(T)$ have already been investigated in [1] and [2], the function $P^{flow}_{gas}(T)$, where the indices "*gas*" or "*g*" stand here for "*Ar*", will be investigated in detail in the present work. To keep the calculations via Eq. (1) and the determination of the material specific quantities from measured temperature-time diagrams manageable, it will be assumed, that:

- All sample material specific quantities are considered to be temperature independent.

3.1 Conduction cooling model

For the sample cooling by pure heat conduction (thermal diffusion) in a static Argon gas atmosphere we obtained in [2] a formula for the power loss in the TEMPUS parabolic flight facility

$$P^{con}_{Ar}(T) = \frac{4\pi a}{1-a/b_{Ar}} \int_{300K}^{T} \lambda_{Ar}(T_{Ar})\, dT_{Ar} \approx \frac{4\pi a}{1-a/b_{Ar}} \lambda_{eff,Ar}\left(T - 300K\right) \tag{3}$$

containing the effective heat transport length $b_{Ar} = 9.55\ mm$. Equation (3) also considers the temperature dependence of the thermal conductivity λ_{Ar} (T_{Ar}) of the Argon gas. It turns out however, see [2, Fig. 10], that in the sample temperature range $1300K \leq T \leq 1700K$, we are interested in, the basically nonlinear sample temperature dependence of the first term on the right hand side of Eq. (3) is very weak and can well be approximated by a linear one with an effective thermal conductivity of the Argon gas of $\lambda_{eff,\,Ar} = 0.042[W/(mK)]$.

3.2 Forced convection cooling model

Forced gas flow or, in other words, convective gas cooling means, that heat from the hot sample is not only transported by conduction (diffusion) through the gas to the cold heat sink of temperature T_∞ but also by an additional movement of the gas heated at the sample surface. The relation between the heat transport by convection ($\approx v_\infty \rho_g c_p T_g$) and the heat transport by conduction ($\approx \lambda_g T_g / R_0$) is given by the dimensionless Péclet number [11]

$$Pe := \frac{v_\infty \rho_g c_p R_0}{\lambda_g} \tag{4}$$

where v_∞, ρ_g, c_p, and λ_g denote the characteristic flow velocity, the mass density, the specific heat (related to the mass) and the thermal conductivity of the gas, respectively, and where $R_o = a$ is the characteristic length scale in the system.

For small Péclet numbers $Pe<<1$, a situation which generally takes place for the thermally well conducting Helium cooling gas or for the thermally poor conducting Argon gas at very low flow velocities, we derived in [3] for the convective term $P_{gas}^{flow}(T)$ of Eq. (2) a formula which is a first order correction to the dominant conductive term $P_{gas}^{con}(T)$. Applied on the thermally very well conducting Helium gas at not too high flow velocities v_∞, this formula described the experimentally measured convective cooling of the Zirconium test sample pretty well [3]. It failed however, when it was applied on the thermally poor conducting Argon gas streaming with about the same flow velocities around the droplet, because the property $\lambda_{Ar} \approx 0.1\ \lambda_{He}$, resulting according to Eq. (4) in $Pe_{Ar} \approx 10 Pe_{He}$, violates in this case the assumption of a small Péclet number.

For high Péclet numbers $Pe >>1$, where the thermal energy, transferred by heat conduction from the droplet surface in normal direction into the poorly conducting Argon gas, is very low, the gas stream quickly blows the heat in tangential direction away as schematically illustrated in Fig. 4. Consequently, the $P_{Ar}^{con}(T)$ term in Eq. (2), describing the radial heat conduction in the Argon cooling gas from the sample of surface temperature T to the heat sink at $T_\infty = 300K$, can at higher Argon flow velocities be neglected compared to the convective term $P_{Ar}^{flow}(T)$. To describe the primarily remaining convective sample cooling $P_{Ar}^{flow}(T)$ by the Argon gas flow at "higher" velocities, i.e., for $Pe >>1$, we apply in the following a physical model, that

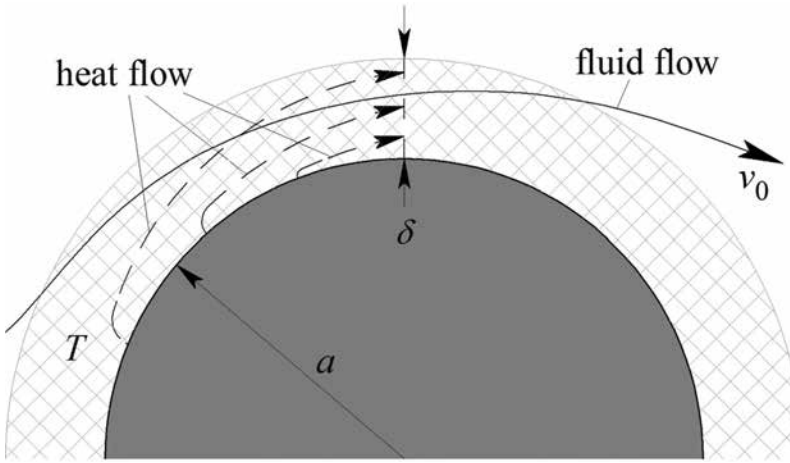

FIGURE 4
Schematic cut showing the fluid flow streaming around a hot sphere (grey) and the resulting heat flow inside the (cross hatched) thermal boundary layer of typical thickness $\delta << a$.

has been derived in [9] for a shear flow of an incompressible cooling fluid along the sample

$$P_{Ar}^{flow}(T) \propto \lambda_{Ar}\, a\, Pe^{1/3}(T-300K) = C_{Ar}\, \tilde{a}^{4/3}\, v_{\infty}{}^{1/3}(T-300K), \qquad (5)$$

where C_{Ar} is an Argon gas specific constant, $\tilde{a} := a$ / 3.5 mm denotes the normalized sample radius, and $300K$ is assumed to be the gas temperature far away from the sample. Although the density of the Argon cooling gas ρ_{Ar}, appearing in Eq. (4) and thus through C_{Ar} also in (5), is temperature dependent and not constant, we will nevertheless use this formula in the following in absence of a better one. We remind, that the condition $Pe >> 1$ also means, that Eq. (5) fails for very low flow velocities v_{∞}.

3.3 Cooling model for the whole flow velocity range

According to the above considerations, the power loss of the sample due to the surrounding Argon atmosphere, given by Eq. (2), can for high flow velocities v_{∞} approximately be described by $P_{Ar}(T) \approx P_{Ar}^{flow}(T)$, where the remaining convective term is given by Eq. (5). For very low flow velocities it can approximately be described by $P_{Ar}(T) \approx P_{Ar}^{con}(T)$, where the remaining conductive term is given by Eq. (3). Since from a physical point of view the sample cooling increases monotonically with increasing flow velocity, we try to cover also the intermediate velocity range by combining the two models via the pure phenomenological construction

$$P_{Ar}(T) \approx P_{Ar}^{con}(T)\exp(-c_v v_{\infty}) + P_{Ar}^{flow}(T)\left(1-\exp(-c_v v_{\infty})\right), \qquad (6)$$

in which the two terms are weighted by the exponential functions dependent on the flow velocity v_{∞}. The occurring parameter c_v has to be determined by a fit of Eq. (6) to experimental data. Explicit insertion of Eq. (3) and (5) in Eq. (6) yields for the levitation system shown in Fig. 2 a physical model for the cooling of a sample by the surrounding Argon atmosphere which is assumed to be valid in the whole velocity range of the gas flow

$$\frac{P_{Ar}(T)}{T-300K} = \begin{pmatrix} \dfrac{4\pi a}{1-a/b_{Ar}}\lambda_{eff,Ar}\exp(-c_v v_{\infty}) \\ +C_{Ar}\,\tilde{a}^{4/3}\, v_{\infty}{}^{1/3}\left(1-\exp(-c_v v_{\infty})\right) \end{pmatrix}\left[\frac{W}{K}\right]. \qquad (7)$$

3.4 Gas flow system

In our present experimental situation, shown in Fig. 2, the gas flow is generated by a gas circulation system. According to the sketch in Fig. 5, the ambient gas of pressure p_{∞} from the process chamber is raised by a rotary pump to the pressure p_p that drives the gas through the tube and the nozzle, consisting

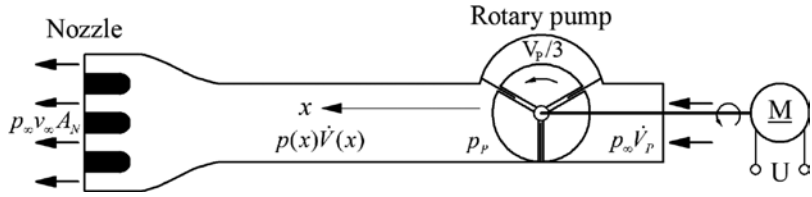

FIGURE 5
Sketch of the gas flow system with the nozzle of total cross section A_N on the one side of the tube, where the gas is blown out with speed v_∞ against the sample in the process chamber of gas pressure p_∞, and with the rotary pump on the other side of the tube, which raises the gas pressure at its outlet from p_∞ to p_P.

of a mesh of thin holes of total cross section A_N, against the sample in the process chamber. For the not directly measurable velocity v_∞ of the uniform gas flow behind the nozzle, which appears in Eq. (7), we derived in [3] a formula, which relates this quantity to the the adjustable input voltage U of the electric pump

$$v_\infty = c_\infty w(\tilde{U}) \quad \text{with} \quad w(\tilde{U}) := \tilde{U} + \tilde{p}_\infty \left(1 + c_g\right)\left(1 - \sqrt{1 + \frac{2c_g}{\left(1+c_g\right)^2}\frac{\tilde{U}}{\tilde{p}_\infty}}\right) \tag{8}$$

where the dimensionless flow velocity $w(\tilde{U})$ is defined as a function of the normalized pump voltage $\tilde{U} := U/1V$, the normalized ambient pressure $\tilde{p}_\infty := p_\infty/350$ mbar, and the gas specific constant c_g. The flow system specific constant c_∞ will merge with the unknown parameters c_v and C_{Ar} of Eq. (7).

4 EXPERIMENTAL RESULTS

To obtain experimentally the sample power loss in the TEMPUS parabolic flight facility for the case, that the levitated sample is processed in an Argon gas atmosphere, we apply Eq. (1) on the cooling ranges of the temperature-time diagrams measured for the Zr test sample during the parabolas No. 1 – No. 5, see Sec. 2. The sum of the induced electrical power input term P^{ind} and the radiation power loss function $P^{rad}(T)$ on the right hand side of Eq. (1), can be obtained, if Eq. (1) is applied on the cooling range of the temperature-time diagram measured for the Zr test sample in vacuum during parabola No. 1, where $P_{Ar}(T) = 0$

$$m c_p \left.\frac{dT(t)}{dt}\right|_{vac} = P^{ind} - P^{rad}(T).$$

Then the measured power loss, caused solely by the surrounding Argon gas in the process chamber, results for our Zr test sample in

$$P_{Ar}(T) = 0.391\left[\frac{Ws}{K}\right]\left(\left.\frac{dT}{dt}(T)\right|_{vac} - \left.\frac{dT}{dt}(T)\right|_{Ar}\right), \tag{9}$$

where its value of mc_p has already been inserted. This measured temperature dependent power loss function $P_{Ar}(T)$ will then be compared with the physical model of Eq. (7) and (8) to check its applicability and to obtain the unknown constants contained in it.

4.1 Cooling in vacuum

The data, resulting from temperature measurements on the solid Zirconium test sphere processed, as described in Sec. 2, in TEMPUS under **vacuum** during the ≈20 seconds μg time of parabola No. 1, are shown in Fig. 6. To obtain for Eq. (9) a reasonable, smooth time derivative from the scattered, but in the mean monotonically decreasing temperature data points of Fig. 6, we fit purely phenomenologically the temperature data by the everywhere monotonically decreasing exponential function

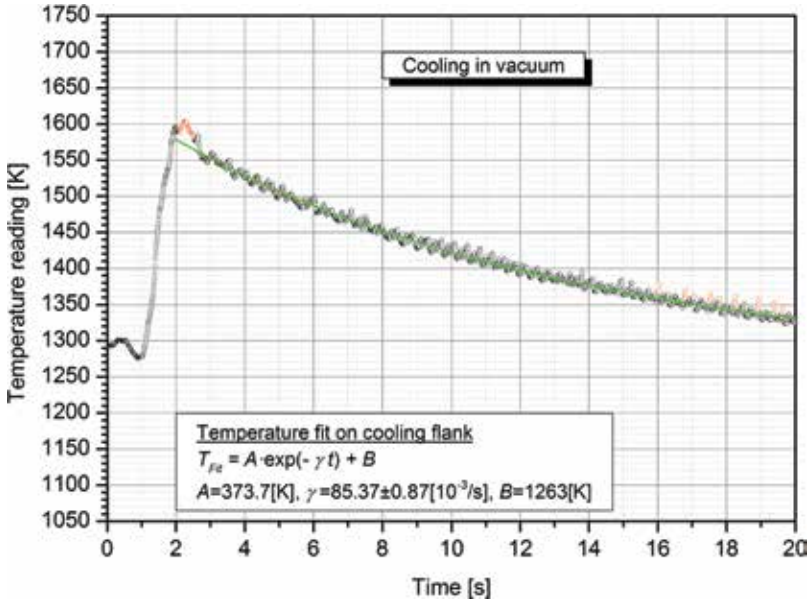

FIGURE 6
Temperature-time profile (black circles) of the solid Zirconium sphere processed in TEMPUS under vacuum during the ≈20s μg time of parabola No. 1. An exponential function (green line) is fitted to the data points of the cooling flank in the temperature range between 1350K and 1600K omitting the red marked runaway points.

$$T(t) = A \cdot \exp\left(-\gamma t\right) + B \tag{10}$$

with the three variable parameters A, γ and B. Evidently this function fits for the parameters shown in the diagram pretty well to the experimental temperature data in the range between 1350K and 1600K. By this procedure the smoothed temperature dependent time derivative of the measured temperature data required for Eq. (9) is simply obtained by the analytical time derivative of the function in Eq. (10)

$$dT/dt\,(T(t)) = -\gamma A \cdot \exp\left(-\gamma t\right) = \gamma\,(B - T(t))\,, \tag{11}$$

which results in a linear function of the temperature T with parameters γ and B following directly from the fit to the temperature data $T(t)$ shown in the diagram.

4.2 Cooling in an Argon gas flow

The diagrams of Fig. 7 show the data resulting from temperature measurements on the solid Zirconium test sphere processed, as described in Sec. 2, in TEMPUS during the ≈20 seconds µg time of the parabolas No. 2 - No.

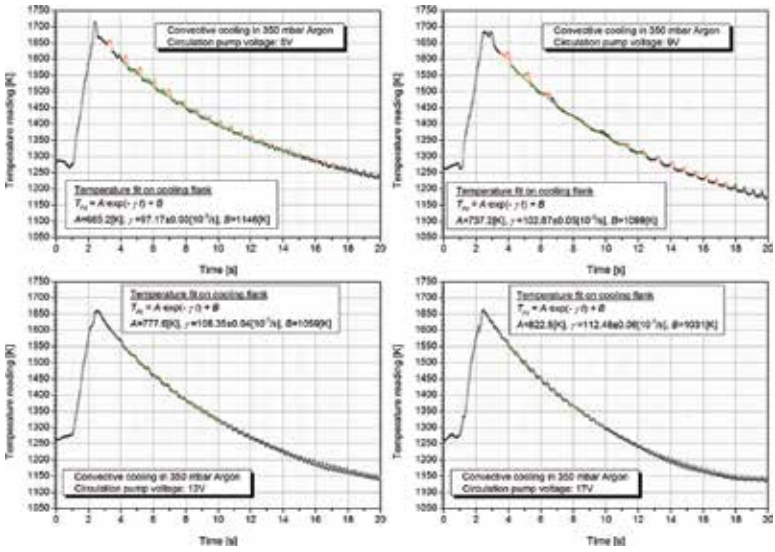

FIGURE 7
Temperature-time profiles (black circles) of the solid Zirconium sphere processed in TEMPUS in a 350 mbar Argon atmosphere during the ≈20s µg time of the parabolas No. 2 to No. 5. Here, the test sphere is additionally exposed to a forced gas flow, the different flow speeds of which result from input voltages of the gas circulation pump of 5V, 9V, 13V and 17V, respectively. Exponential functions (green line) are fitted to the data points of the cooling flank in the temperature range between 1300K and 1600K omitting the red marked runaway points. The fit function properties are shown in the diagrams.

5 in a 350 mbar Argon atmosphere. During these parabolas the test sphere was additionally exposed to a forced Argon **gas flow**, the different flow speeds of which resulted from different voltages applied to the gas circulation pump. Here too, the scattered temperature data of the diagrams in Fig. 7 have been fitted on its cooling flank by the exponential function of Eq. (10) to which we however additionally imposed the constraint

$$\gamma_{flow}(B_{flow} - 300K) = \gamma_{vac}(B_{vac} - 300K) = 82.21[Ks^{-1}] \tag{12}$$

between the fit parameters γ_{flow} and B_{flow}. The number on the right hand side follows from the parameters of the fit to the vacuum cooling data shown in Fig. 6. As we will see below, this condition ensures the linear sample temperature dependence $P_{Ar}(T) \propto T - 300K$ required by the gas cooling model (7). Even subjected to this additional condition, the exponential function of Eq. (10) fits the data of all four flow cooling diagrams in Fig. 7 pretty well thereby confirming this linear sample temperature dependence.

The exponential form of the fit function (10) simplifies the determination of the temperature dependent power loss caused by the Argon atmosphere defined in Eq. (9). Under consideration of Eq. (11) it results for the test sample in

$$\begin{aligned} P_{Ar}(T) &= 0.391\left[Ws/K\right]\left(\gamma_{vac}B_{vac} - \gamma_{flow}B_{flow} + (\gamma_{flow} - \gamma_{vac})T\right) \\ &= 0.391\left[Ws/K\right]\left(\gamma_{flow} - \gamma_{vac}\right)\left(T - 300K\right), \end{aligned} \tag{13}$$

where the second term results from the application of the constraint (12). Insertion of the values for the fit function parameter γ, shown in the diagrams, yields in the temperature range between 1300 K and 1600 K the measured power losses of our Zr test sample caused by forced flow cooling in Argon at gas pump voltages of 5V, 9V, 13V and 17V

$$\begin{aligned} P_{Ar}^{5V}(T) &= 4.61 \pm 0.35\left[\frac{10^{-3}W}{K}\right]\left(T - 300K\right), \\ P_{Ar}^{9V}(T) &= 6.84 \pm 0.36\left[\frac{10^{-3}W}{K}\right]\left(T - 300K\right), \\ P_{Ar}^{13V}(T) &= 8.98 \pm 0.36\left[\frac{10^{-3}W}{K}\right]\left(T - 300K\right), \\ P_{Ar}^{17V}(T) &= 10.7 \pm 0.36\left[\frac{10^{-3}W}{K}\right]\left(T - 300K\right). \end{aligned} \tag{14}$$

4.3 Comparison with the physical model

Essentially two properties of our theoretical gas flow cooling model (7), describing the heat loss from the sample by a forced Argon gas flow, have to be checked in the present paper at hand of the measured values:

1. Besides $P_{Ar}^{con}(T)$ also $P_{Ar}^{flow}(T) \propto T - 300K$ is linearly dependent on the sample temperature T.
2. The dependence of $P_{Ar}(T)$on the flow velocity v_∞ is that of Eq. (7), where v_∞ is given by Eq. (8).

The first property of our theoretical gas flow cooling model (7) has already very well been confirmed by the results of the preceding section.

In order to check the second property and to find for the TEMPUS facility the unknown parameters in the sample cooling model (7), we compare it for different Argon flow velocities v_∞ with the experimental data presented in Eq. (14). With the effective thermal conductivity $\lambda_{eff,\,Ar} = 0.042[W/(mK)]$ of the Argon gas and the value of the TEMPUS facility specific constant $b_{Ar} = 9.55$ *mm*, noted in Sec. 3.1, and under consideration of the experimental conditions applied during the tests (see above), where the sample radius was $a =$ 3.5 mm ($\Rightarrow \tilde{a} = 1$) and the Argon pressure p_∞ = 350 mbar ($\Rightarrow \tilde{p}_\infty$ = 1), the basic physical model, consisting of Eq. (7) and (8), results in

$$\frac{P_{Ar}^{\tilde{U}}(T)}{T-300K} = \begin{pmatrix} 2.92\cdot 10^{-3}\exp(-c_{v1}w(\tilde{U})) \\ +C_{Ar1}w(\tilde{U})^{1/3}\left(1-\exp\left(-c_{v1}w(\tilde{U})\right)\right) \end{pmatrix}\left[\frac{W}{K}\right] \tag{15}$$

with the fit parameters C_{Ar1} and c_{v1}, and the dimensionless flow velocity

$$w(\tilde{U}) = \tilde{U} + 41.8\left(1-\sqrt{1+0.0467\tilde{U}}\right) \tag{16}$$

depending on the normalized pump voltage $\tilde{U}$:=U / *1V*. In calculating Eq. (16) we applied for the gas viscosity dependent constant $c_{Ar} \approx c_{He} = 40.8$ that value which has already been found in [3] for the Helium gas, because the viscosities of Argon and Helium gas are very similar. In Fig. 8 the 4 measurement data for $P_{Ar}(T)$ / $(T - 300K)$, listed in Eq. (14), which belong to the gas pump voltages of U = 5V, 9V, 13V and 17V, respectively, have been plotted against the values of the normalized Argon gas velocity $w(U)$. The solid curve in the diagram of Fig. 8 reflects the best fit of the function of Eq. (15) to the data points for variable parameters C_{Ar1} and c_{v1}. It takes place for

$$C_{Ar1} = 7.45\cdot 10^{-3} \text{ and } c_{v1} = 2.51.$$

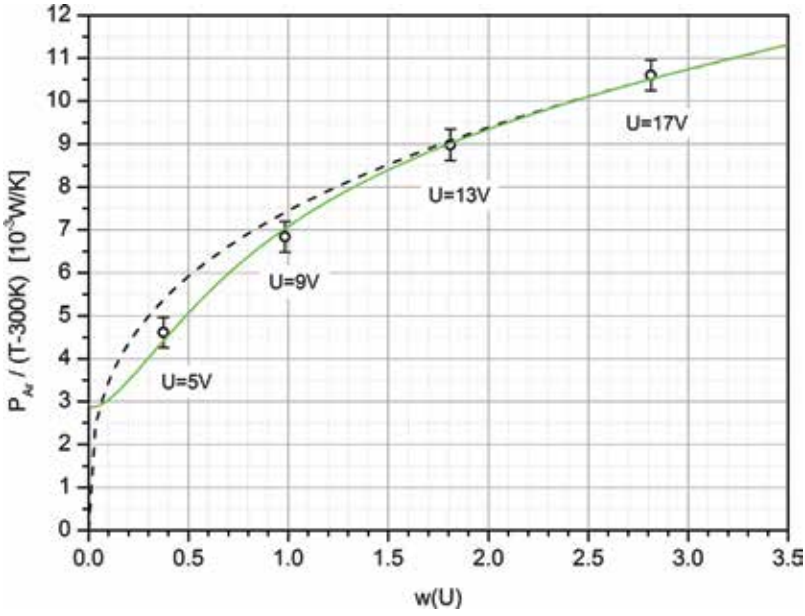

FIGURE 8
Temperature normalized power loss by forced convection from the solid $\varnothing = 7$ mm Zirconium test sphere, levitated in TEMPUS in a 350 mbar Argon atmosphere. The measurement data points from Eq. (14) (black circles) belong to the dimensionless gas flow velocities $w(U)$ which result from gas pump voltages of 5V, 9V, 13V and 17V, respectively. The solid curve is the best fit of the function on the right hand side of Eq. (15) to the data points. The dashed curve reflects the model of Eq. (5).

The good coincidence of the model of Eq. (15) with the experimental data confirms also the second property. The dashed curve in in the diagram of Fig. 8 is the graph of $7.45 \cdot 10^{-3} \cdot w(U)^{1/3}$, which, according to Sec. 3.2, represents the sample cooling model for the high gas flow velocities.

5 SUMMARY

To describe the forced convective cooling of an isothermal sphere of temperature T and radius a, levitated in the centre of a coil system as illustrated in Fig. 2, and exposed to an additional Argon gas flow, we derived for the sample power loss in the whole flow velocity range the relation

$$\frac{P_{Ar}(T)}{T-300K} = \left(\begin{array}{l} \dfrac{4\pi a}{1-a/b_{Ar}} \lambda_{eff,Ar} \exp(-c_v v_\infty) \\ +C_{Ar}\, \tilde{a}^{4/3}\, {v_\infty}^{1/3} \left(1-\exp(-c_v v_\infty)\right) \end{array} \right) \left[\frac{W}{K}\right]. \qquad (7)$$

The parameter b_{Ar} and the effective Argon conductivity $\lambda_{eff,Ar}$ are explained in Sec. 3.1, $\tilde{a} = a/3.5$ mm denotes the normalized sample radius, v_∞ is the velocity of the uniform gas flow, and C_{Ar} is a gas type specific constant that has to be determined experimentally by a fit to measurement values. The two terms of Eq. (7), where the first one describes the sample power loss by heat conduction in the Argon gas only, and the second one only the power loss by forced convection at high gas flow velocities v_∞, have phenomenologically been combined by the exponential weighting functions containing the flow system specific fit parameter c_v.

In our present experimental situation the gas flow is generated by a circulation pump driving the gas from the experiment chamber through a nozzle against the sample, see Fig. 2. The relation between the velocity v_∞ of the uniform gas flow, appearing in Eq. (7), and the adjustable input voltage U of the electric pump is given by [3]

$$v_\infty = c_\infty w(\tilde{U}) \quad \text{with} \quad w(\tilde{U}) := \tilde{U} + \tilde{p}_\infty \left(1 + c_{Ar}\right)\left(1 - \sqrt{1 + \frac{2\,c_{Ar}}{\left(1 + c_{Ar}\right)^2}\frac{\tilde{U}}{\tilde{p}_\infty}}\right), \tag{8}$$

where the dimensionless flow velocity $w(\tilde{U})$ is defined as a function of the normalized pump voltage $\tilde{U} := U\ /\ 1V$, the normalized ambient pressure $\tilde{p}_\infty := p_\infty/350$ mbar , and the gas specific constant c_{Ar}.

Especially for the TEMPUS levitation facility with the already in [2] and [3] determined values of $b_{Ar} = 9.55\ mm$, $\lambda_{eff,Ar} = 0.042\ [W/(mK)]$ and $c_{Ar} \approx c_{He} = 40.8$, the sample power loss (7) caused by the streaming Argon atmosphere results in

$$\frac{P_{Ar}^{\tilde{U}}(T)}{T - 300K} = \begin{pmatrix} \dfrac{1.85\cdot 10^{-3}\,\tilde{a}}{1 - 0.366\,\tilde{a}}\exp(-c_{v1}\,w(\tilde{U})) \\ +C_{Ar1}\,\tilde{a}^{4/3}\,w(\tilde{U})^{1/3}\left(1 - \exp(-c_{v1}\,w(\tilde{U}))\right) \end{pmatrix}\left[\frac{W}{K}\right] \tag{17}$$

with

$$w(\tilde{U}) = \tilde{U} + 41.8\,\tilde{p}_\infty\left(1 - \sqrt{1 + 0.0467\,\tilde{U}/\tilde{p}_\infty}\right) \tag{18}$$

To check the above models for the sample power loss in Argon, we measured the temperature time behaviour of a solid spherical Zirconium sample levitated in TEMPUS under different atmospheric conditions (static Argon gas, forced Argon gas flow at different pump voltages) within the $\approx$20 seconds weightlessness time of several parabolas flown during a parabolic flight mission of TEMPUS. A sketch of the sample and its environment is shown in Fig. 2. Due to the weightlessness the otherwise additionally occurring natural

convection cooling in the surrounding gas atmosphere didn't occur. It turned out, that our forced convection model of Eq. (17) and (18) fits very well to the measured heat loss of our levitated test sample in the streaming Argon atmosphere, if the TEMPUS facility specific constants C_{Ar1} and c_{v1} assume the values

$$C_{Ar1} = 7.45 \cdot 10^{-3} \text{ and } c_{v1} = 2.51.$$

Together with the results for the induced electrical power $P^{ind}(t)$ and the power loss by radiation $P^{rad}(T(t))$, derived in [1] and [2], Eq. (17) and (18) complete the heat balance equation

$$\frac{dE(t)}{dt} = m\,c_p\,\frac{dT(t)}{dt} = P^{ind}(t) - P^{rad}(T(t)) - P_{gas}(T(t))\,, \tag{1}$$

which, after a numerical integration, allows to predict with sufficient accuracy the temperature-time behaviour of a sample levitated in the TEMPUS facility.

ACKNOWLEDGMENTS

The authors thank the space agency of the "German Aerospace Center" (DLR), Bonn for enabling us to perform the experiments during the 25th DLR parabolic flight campaign 2014. Furthermore, they thank the pilots and crew members of "Novespace", Bordeaux for the almost jitter-free execution of the parabolic flights and the members of the TEMPUS team for the operation of the TEMPUS facility.

REFERENCE

[1] G. Lohöfer and I. Egry, *High Temp. - High Press.* 42, (2013), 175–202.
[2] G. Lohöfer and S. Schneider, *High Temp. - High Press.* 44, (2015), 147–162.
[3] G. Lohöfer and S. Schneider, *High Temp. - High Press.* 44, (2015), 429–450.
[4] J. Brillo, G. Lohöfer, F. Schmidt-Hohagen, S. Schneider and I. Egry, *Int. J. Materials and Product Technology* 26, (2006), 247–273.
[5] D. Herlach, R. Cochrane, I. Egry, H. Fecht and L. Greer, *International Materials Review* 38, (1993), 273–347.
[6] *25th DLR Parabolic flight campaign, 20th–31st October 2014, Practical and Technical Information*, DI-2014-ed1-en, Novespace, Bordeaux-Mérignac, Mars 2014. See also: www.novespace.com
[7] I. Egry and D. Voss, *JASMA* 27, (2010), 178–182.
[8] G. Lohöfer and J. Piller, Proc. 40th AIAA Aerospace Sciences Meeting & Exhibit, 14–17. January 2002, Reno, U.S.A, paper no.: AIAA 2002–0764.
[9] G. Lohöfer, *Int. J. Thermal Sciences*, to appear (2016).
[10] N. D. Milosevic and K.D. Maglic, *Int. J. Thermophys.* 27, (2006), 1140–1159.
[11] E. Guyon, J.-P. Hulin, L. Petit and C. D. Mitescu, *Physical Hydrodynamics*, Oxford University Press, New York, 2001.